LOCKHEED MARTIN ENERGY RESEARCH LIBRARIES
3 4456 0515409 8

ORNL-4805

Cy 1

NITROGEN NEUTRON ELASTIC AND INELASTIC SCATTERING CROSS SECTIONS FROM 4.34 TO 8.56 MeV

F. G. Perey
W. E. Kinney

OAK RIDGE NATIONAL LABORATORY
CENTRAL RESEARCH LIBRARY
DOCUMENT COLLECTION
LIBRARY LOAN COPY
DO NOT TRANSFER TO ANOTHER PERSON
If you wish someone else to see this document, send in name with document and the library will arrange a loan.

OAK RIDGE NATIONAL LABORATORY
OPERATED BY UNION CARBIDE CORPORATION • FOR THE U.S. ATOMIC ENERGY COMMISSION

Printed in the United States of America. Available from
National Technical Information Service
U.S. Department of Commerce
5285 Port Royal Road, Springfield, Virginia 22151
Price: Printed Copy $4.00; Microfiche $0.95

This report was prepared as an account of work sponsored by the United States Government. Neither the United States nor the United States Atomic Energy Commission, nor any of their employees, nor any of their contractors, subcontractors, or their employees, makes any warranty, express or implied, or assumes any legal liability or responsibility for the accuracy, completeness or usefulness of any information, apparatus, product or process disclosed, or represents that its use would not infringe privately owned rights.

ORNL-4805
UC-79d
(ENDF-205)

Contract No. W-7405-eng-26

Neutron Physics Division

NITROGEN NEUTRON ELASTIC AND INELASTIC SCATTERING CROSS SECTIONS FROM 4.34 TO 8.56 MeV

F. G. Perey and W. E. Kinney

FEBRUARY 1974

OAK RIDGE NATIONAL LABORATORY
Oak Ridge, Tennessee 37830
operated by
UNION CARBIDE CORPORATION
for the
U.S. ATOMIC ENERGY COMMISSION

LOCKHEED MARTIN ENERGY RESEARCH LIBRARIES
3 4456 0515409 8

CONTENTS

Abstract 1

Introduction 1

Data Acquisition 1

Data Reduction 2

Results 4

Elastic Scattering Differential Cross Sections 4

Inelastic Scattering Differential Cross Sections 11

Excitation Functions 11

Conclusions 14

Acknowledgments 14

References 15

Appendix 17

NITROGEN NEUTRON ELASTIC AND INELASTIC SCATTERING CROSS SECTIONS FROM 4.34 TO 8.56 MeV

F. G. Perey and W. E. Kinney

ABSTRACT

Measured nitrogen neutron elastic and inelastic cross sections at incident neutron energies from 4.34 to 8.56 MeV are presented and compared with previous results. Our elastic data are systematically lower than the data of Bostrum et al. and systematically higher than the data of Bauer et al. but generally agree with the data of Chase et al. and Phillips. Our angle-integrated differential inelastic scattering cross sections are in reasonable agreement with previous results. Agreement of our data and ENDF/B III MAT 1133 is reasonable.

INTRODUCTION

The data reported here are the results of one of a series of experiments to measure neutron elastic and inelastic scattering cross sections at the ORNL Van de Graaffs. Reports in the series are listed in Reference 1. This report presents measured neutron elastic and inelastic scattering cross sections for nitrogen from 4.34 to 8.56 MeV. To assist in the evaluation of the data, the data acquisition and reduction techniques are first briefly discussed. For the purposes of discussion the data are presented in graphical form and are compared with the results of others and with ENDF/B III (Evaluated Neutron Data File B, Version III) MAT 1133. Tables of numerical values of the elastic scattering cross sections and cross sections for inelastic scattering to discrete levels in the residual nucleus are given in an appendix.

DATA ACQUISITION

The data were obtained with conventional time-of-flight techniques. Pulsed (2 MHz), bunched (approximately 1.5 nsec full width at half maximum, FWHM) deuterons accelerated by the ORNL Van de Graaffs interacted with deuterium in a gas cell to produce neutrons by the $D(d,n)^3He$ reaction. The gas cells, of length 1 and 2 cm, were operated at pressures of approximately 1.5 atm and gave neutron energy resolutions of the order of ± 60 keV.

The neutrons were scattered from a solid right circular cylindrical sample of ammonium azide NH_4N_3 contained in a 0.254 mm thick stainless steel can 1.943 in. in diameter and 2.667 cm in height. The mass of ammonium azide was 4.85 gm.

The scattered neutrons were detected by 12.5 cm diameter NE-213 liquid scintillators optically coupled to XP-1040 photomultipliers. The scintillators were 2.5 cm thick. Data were taken with three detectors simultaneously. Flight paths were approximately 4 m with

the detector angles ranging from 15 to 140 degrees. The gas cell neutron production was monitored by a time-of-flight system which used a 5 cm diameter by 2.5 cm thick NE-213 scintillator viewed by a 56-AVP photomultiplier placed about 4 m from the cell at an angle of 55 degrees with the incident deuteron beam.

For each event a PDP-7 computer was given the flight time of a detected recoil proton event with reference to a beam pulse signal, the pulse height of the recoil proton event, and identification of the detector. The electronic equipment for supplying this information to the computer consisted, for the most part, of standard commercial components. The electronic bias was set at approximately 700 keV neutron energy to ensure good pulse shape discrimination against gamma-rays at all energies.

The detector efficiencies were measured by (n,p) scattering from a 6 mm diameter polyethylene sample and by detecting source $D(d,n)^3He$ neutrons at 0 degrees[3]. Both interactions gave results which agreed with each other and which yielded efficiency versus energy curves that compared well with calculations[4].

DATA REDUCTION

Central to the data reduction process was the use of a light pen with the PDP-7 computer oscilloscope display programs to extract peak areas from spectra. The light pen made a comparatively easy job of estimating errors in the cross section caused by extreme but possible peak shapes.

The reduction process started by normalizing a sample-out to a sample-in time-of-flight spectrum by the ratio of their monitor neutron peak areas, subtracting the sample-out spectrum, and transforming the difference spectrum into a spectrum of center-of-mass cross section versus excitation energy. This transformation allowed ready comparison of spectra taken at different angles and incident neutron energies by removing kinematic effects. It also made all single peaks have approximately the same shape and width regardless of excitation energy (in a time-of-flight spectrum, single peaks broaden with increasing flight time). A spectrum of the variance based on the counting statistics of the initial data was also computed. Figure 1 shows a typical time-of-flight spectrum and its transformed energy spectrum.

The transformed spectra were read into the PDP-7 computer and the peak stripping was done with the aid of the light pen. A peak was stripped by drawing a background beneath it, subtracting the background, and calculating the area, centroid, and FWHM of the difference. The variance spectrum was used to compute a counting statistics variance corresponding to the stripped peak. Peak stripping errors due to uncertainties in the residual background under the peaks or to the tails of imperfectly resolved nearby peaks could be included with the other errors by stripping the peaks several times corresponding to high, low, and best estimates of this background. Although somewhat subjective, the low and high estimates of the cross sections were identified with 95% confidence limits; these, together with the best estimate, defined upper and lower errors due to stripping. When a spectrum was completely stripped, the output information was written on magnetic tape for additional processing by a large computer.

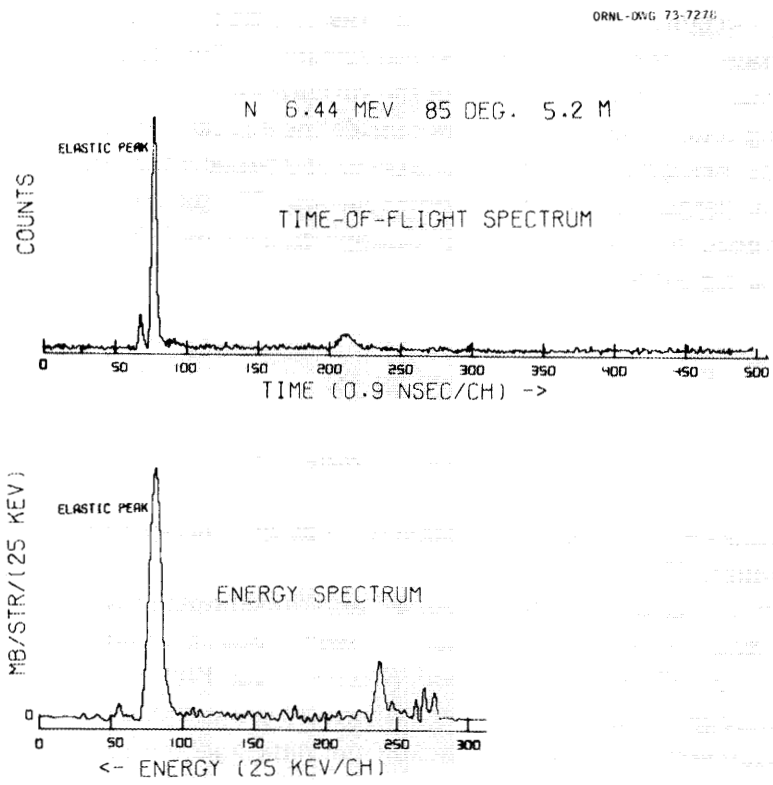

Fig. 1. A typical time-of-flight spectrum for nitrogen with its transformed energy spectrum. The data were taken at 6.0 MeV incident neutron energy at an angle of 90 deg. with a 4 m flight path. Note that the energy spectrum has been offset to allow negative excursions due to statistics in the subtraction of the sample-out background.

Finite sample corrections were performed according to semianalytic recipes whose constants were obtained from fits to Monte Carlo results.[4] The corrections were less than 5%.

The final error analysis included uncertainties in the geometrical parameters (scatterer size, gas cell-to-scatterer distance, flight paths, etc.) and uncertainties in the finite sample corrections.

The measured differential elastic scattering cross sections were fitted by least squares to a Legendre series:

$$\sigma(\mu = \cos\theta) = \Sigma[(2k+1)/2)]a_k P_k(\mu)$$

the points being weighted by the inverse of their variances which were computed by squaring the average of the upper and lower uncertainties. The common 7% uncertainty in absolute normalization was not included in the variances for the fitting. In order to prevent the fit from giving totally unrealistic values outside the angular range of our measurements, we resorted to the inelegant but workable process of adding three points equally spaced in angle between the largest angle of measurement and 175 degrees. The differential cross sections at the added points were chosen to approximate the diffraction pattern at large angles, but were assigned 50% errors.

RESULTS

Elastic Scattering Differential Cross Sections

Our differential elastic scattering cross sections are shown in Figures 2 and 3 with Legendre least squares fits to the data.

Our differential elastic scattering cross sections are compared with the results of others in Figures 4, 5, and 6. The other investigators whose data are shown are Bostrom, et al. (BOS+),[5] Chase et al. (CHA+)[6], Bauer et al. (BAU+)[7], and Phillips (PHIL)[8]. Their energies of measurement are given in Table I. In the figures, when our data (ORNL) are given, our energies of measurement are used in labeling the data and the data of others at nearby energies which are compared.

The angular distributions from ENDF/B III MAT 1133 are also shown in Figures 4, 5, and 6. They are normalized to integrals of the experimental data. When other sets of data are compared with ours at the same energies, our integrals were used to normalize the ENDF/B angular distributions.

Nitrogen, as do other light nuclei, shows resonant structure in its total cross section in the 4 to 9 MeV energy region[9], with peaks falling at roughly 4.2, 4.6, 7.4, and 7.8 MeV. One would expect the elastic differential cross sections to be affected by resonant structure so that in Figures 4, 5, and 6 one should be prepared for differences in shapes of the angular distributions at adjacent energies of measurement near the resonance energies. In fact, our data at 4.92 MeV are more nearly isotropic than either our 4.34 or 6.01 MeV data.

Overall, our data are systematically lower than the data of Bostrom, et al. while our data are in reasonably good agreement with the data of Chase, et al. and with Phillips at 7 MeV. Our data agree within experimental uncertainties with the data of Bauer et al. at 8.04

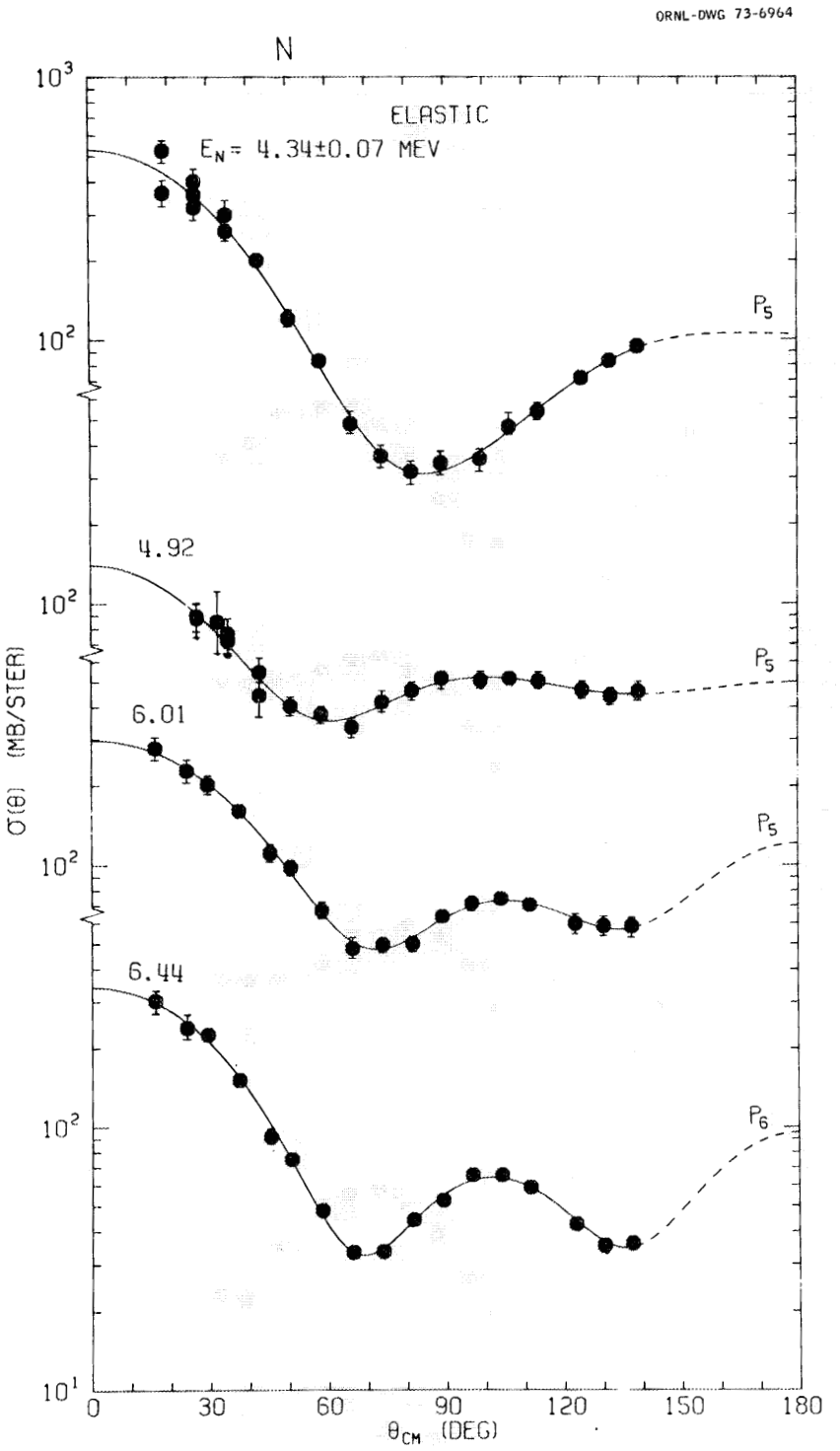

Fig. 2. Our nitrogen neutron differential elastic center-of-mass scattering cross sections with Legendre fits to the data. The 7% uncertainty in absolute normalization common to all points is not included in the error bars.

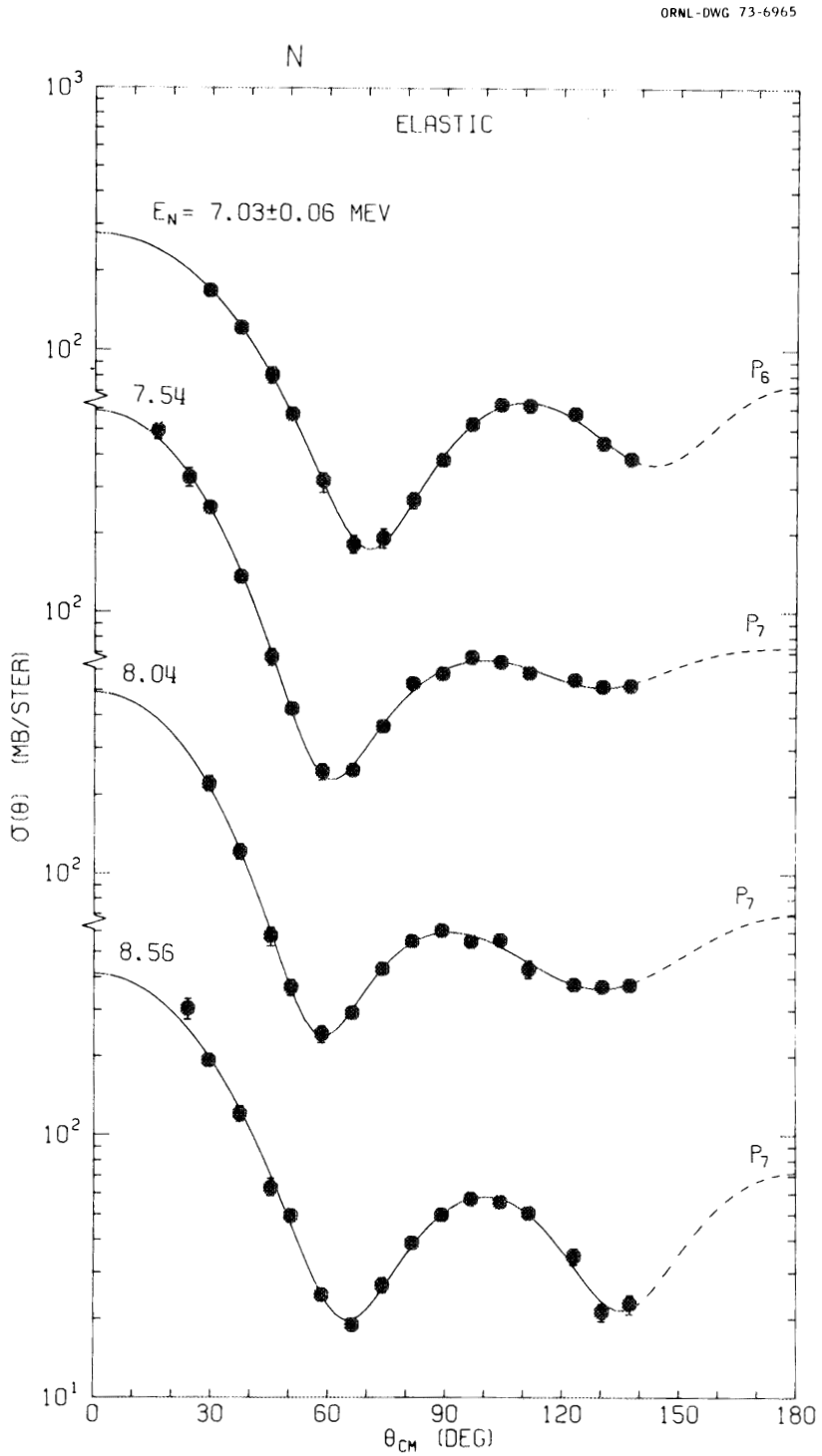

Fig. 3. Our nitrogen neutron differential elastic center-of-mass scattering cross sections with Legendre fits to the data. The 7% uncertainty in absolute normalization common to all points is not included in the error bars.

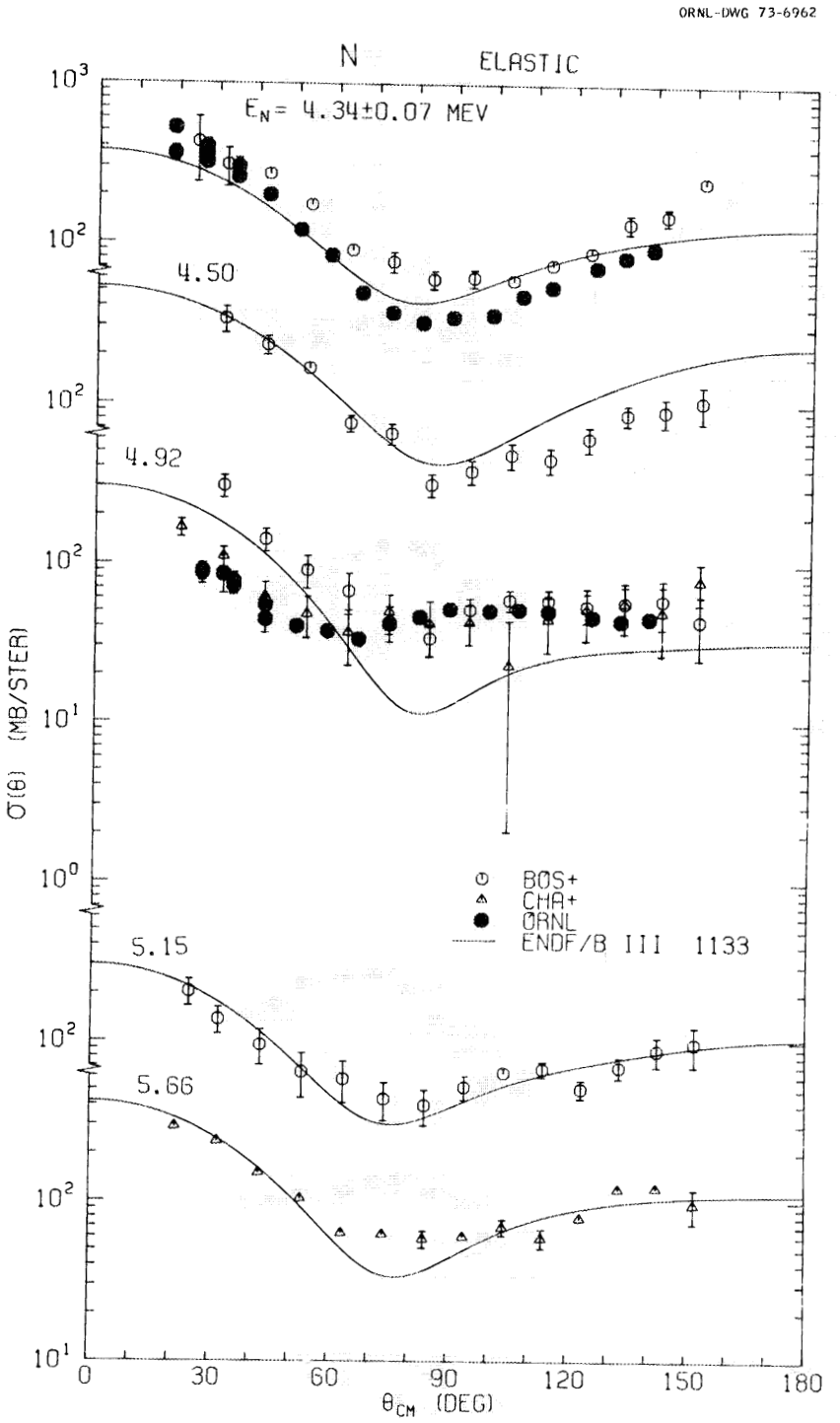

Fig. 4. Our nitrogen neutron differential elastic center-of-mass scattering cross sections compared with the data of Bostrom et al.[5] (BOS+), Chase et al.[6] (CHA+), and with ENDF/B III MAT 1133.

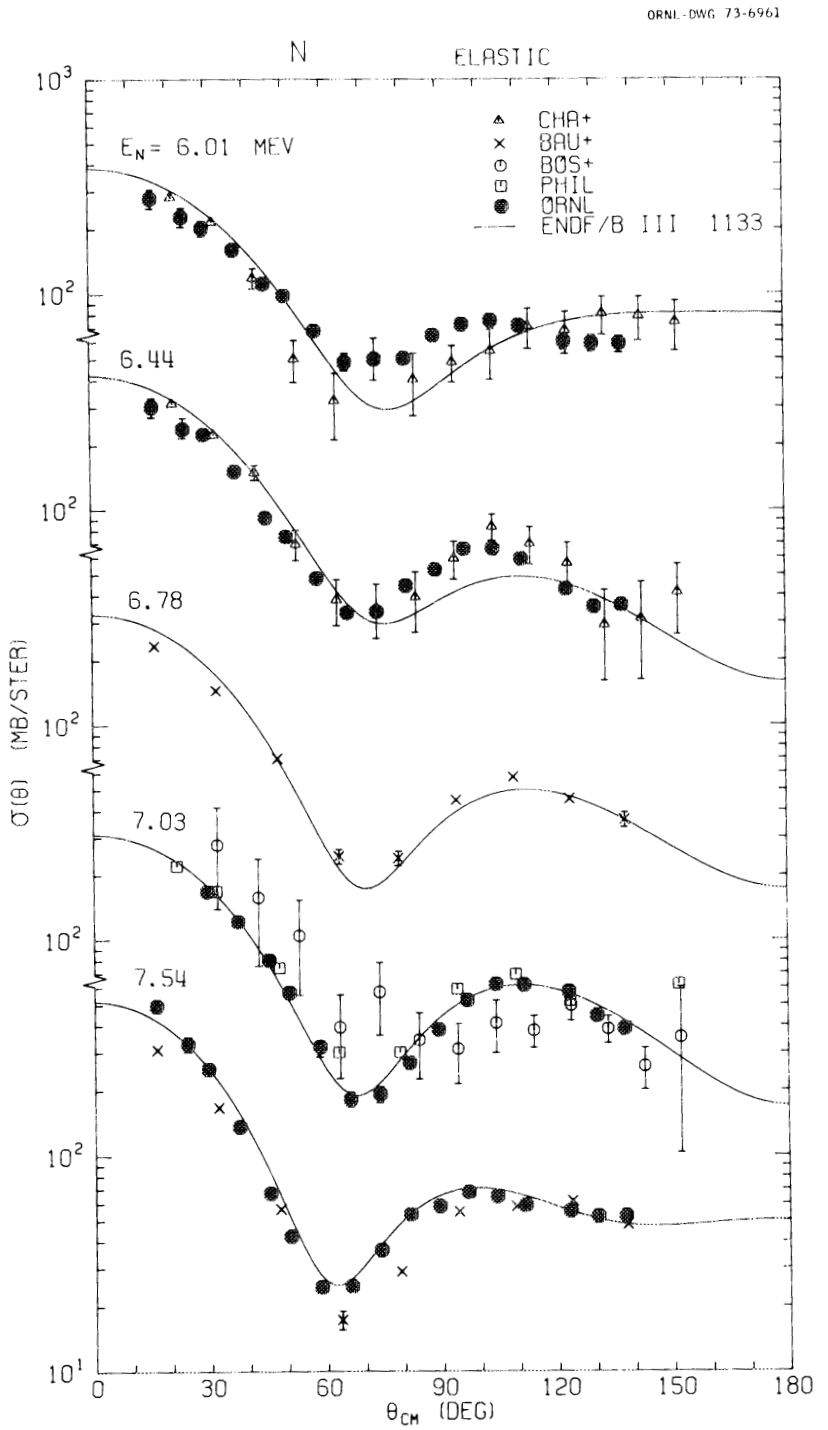

Fig. 5. Our nitrogen neutron differential elastic center-of-mass scattering cross sections compared with the data of Chase et al.[6] (CHA+), Bauer et al.[7] (BAU+), Bostrom et al.[5] (BOS+), and Phillips[8] (PHIL), and with ENDF/B III MAT 1133.

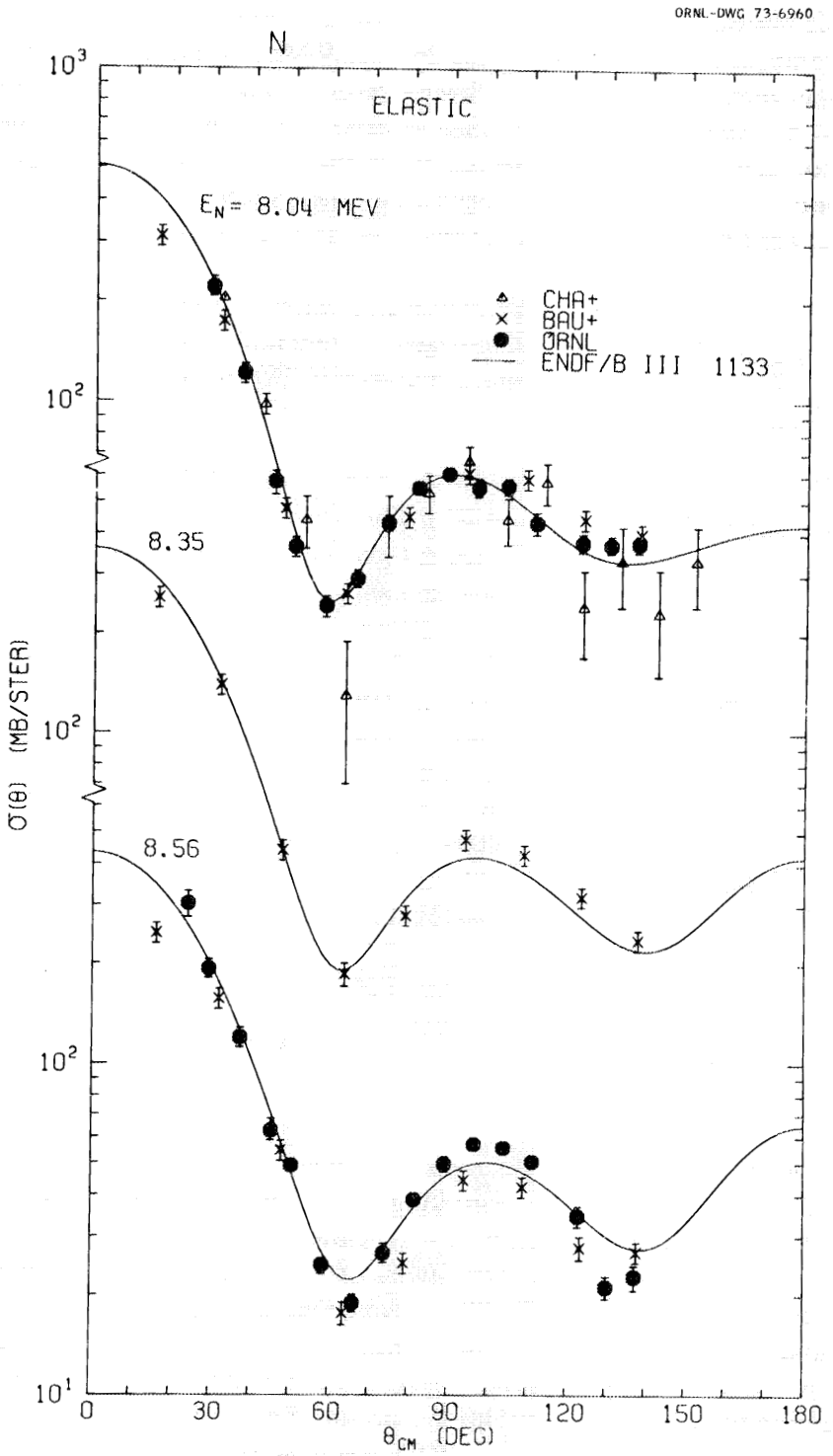

Fig. 6. Our nitrogen neutron differential elastic center-of-mass scattering cross sections compared with the data of Chase et al.[6] (CHA+) and Bauer et al.[7] (BAU+), and with ENDF/B III MAT 1133.

MeV but are systematically higher than theirs at 7.54 and 8.56 MeV. Our energy spreads are ±0.06 MeV compared to the spreads of ±0.26 to 0.29 MeV of Bauer et al. This, and the different energies of measurement in the 7 - 8 MeV resonant region might account for some of the differences but the total cross section is relatively smooth[9] at 8.5 ± 0.3 MeV. The small angle data of Bauer et al. seem to be relatively smaller than our small angle data, but this cannot account for the so-called "nitrogen non-elastic discrepancy"[10] since increasing their two most forward points by 10% raises the integral by only 4%.

Table I. The energies of measurements of other investigators whose nitrogen differential elastic scattering cross sections are shown in Figures 4, 5, and 6.

Investigators	Energies, MeV	References
Bostrom, *et al.*	4.30 ± 0.06	5
	4.50 ± 0.06	
	4.85 ± 0.06	
	5.15 ± 0.06	
	7.11 ± 0.06	
Chase, *et al.*	4.99 ± 0.19	6
	5.66 ± 0.145	
	6.02 ± 0.13	
	6.53 ± 0.115	
	8.00 ± 0.32	
Bauer, *et al.*	6.78 ± 0.30	7
	7.41 ± 0.29	
	7.93 ± 0.27	
	8.35 ± 0.26	
	8.57 ± 0.25	
Phillips	7.0	8

The ENDF/B III MAT 1133 angular distributions, having used the previous elastic data in the evaluation of its elastic scattering, is in generally good agreement with experiment so it is of interest to compare our data with the ENDF/B distributions. Agreement from 7 to 8 MeV is good with most of our data lying within experimental uncertainties of the ENDF/B III MAT 1133 curves. Our data depart at 8.56 MeV in the first minimum and beyond though the forward peak is in reasonably good agreement. At 6.01 and 6.44 MeV our data tend to display less forward peaking but a more pronounced second maxima than the ENDF/B distributions display. This trend is carried to an extreme at 4.92 MeV where our data are comparatively flat. At 4.34 MeV our forward peak is larger than ENDF/B but our data are lower beyond 60 deg. The total cross section shows a broad minimum at roughly 4.9 MeV[9] and the resonance structure may in part be responsible for the differences.

Inelastic Scattering Differential Cross Sections

Our differential cross sections for inelastic scattering to the 3.945 MeV levels are shown in Figure 7. Within experimental uncertainties, they are isotropic.

Excitation Functions

Our angle-integrated differential cross sections as a function of incident neutron energy are shown in Figure 8. The angle-integrated differential elastic scattering cross sections of the other investigators listed in Table I are also shown along with curves from ENDF/B III MAT 1133. The angle-integrated differential inelastic scattering cross sections are compared with previously reported gamma ray data of Dickens and Perey[11] (D+P1), Dickens and Perey[12] (D+P2), and Dickens, Love, and Morgan[13] (DLM). As noted above, our elastic data are systematically lower than the data of Bostrom et al., while there is general agreement among our data and the data of Chase et al. and Phillips. Systematically lower values of Bauer et al., except at 8 MeV, are seen in the figure. Five of our eight elastic points lie within experimental uncertainties of the ENDF/B III MAT 1133 curve notwithstanding the differences in the elastic differential cross sections noted above.

Our data for inelastic scattering to the 3.945 MeV level are in excellent agreement with the gamma ray data above 7 MeV but below 7 MeV are 25 - 30% higher. Our data for inelastic scattering to the 4.910 MeV level lie between the broad resolution NaI gamma ray data (DLM) and the Ge(Li) data (D+P1). Our data for inelastic scattering to the 5.100 MeV level agree within experimental uncertainties with the (DLM) data but are 28% higher than the (D+P1) and (D+P2) results at 8.5 MeV.

Our angle-integrated differential cross sections for inelastic scattering to the 3.945 MeV level are in good agreement with the ENDF/B III curve above 7 MeV though our data lie above the curve at lower energies. Our cross sections for inelastic scattering to the higher levels are in reasonable agreement with ENDF/B III at 7.54 and 8 MeV but are high by a factor of 2 to 3 at 8.5 MeV. ENDF/B III MAT 1133 utilized the data of Dickens and Perey in its evaluation of scattering to these levels.

ORNL-DWG 73-6963

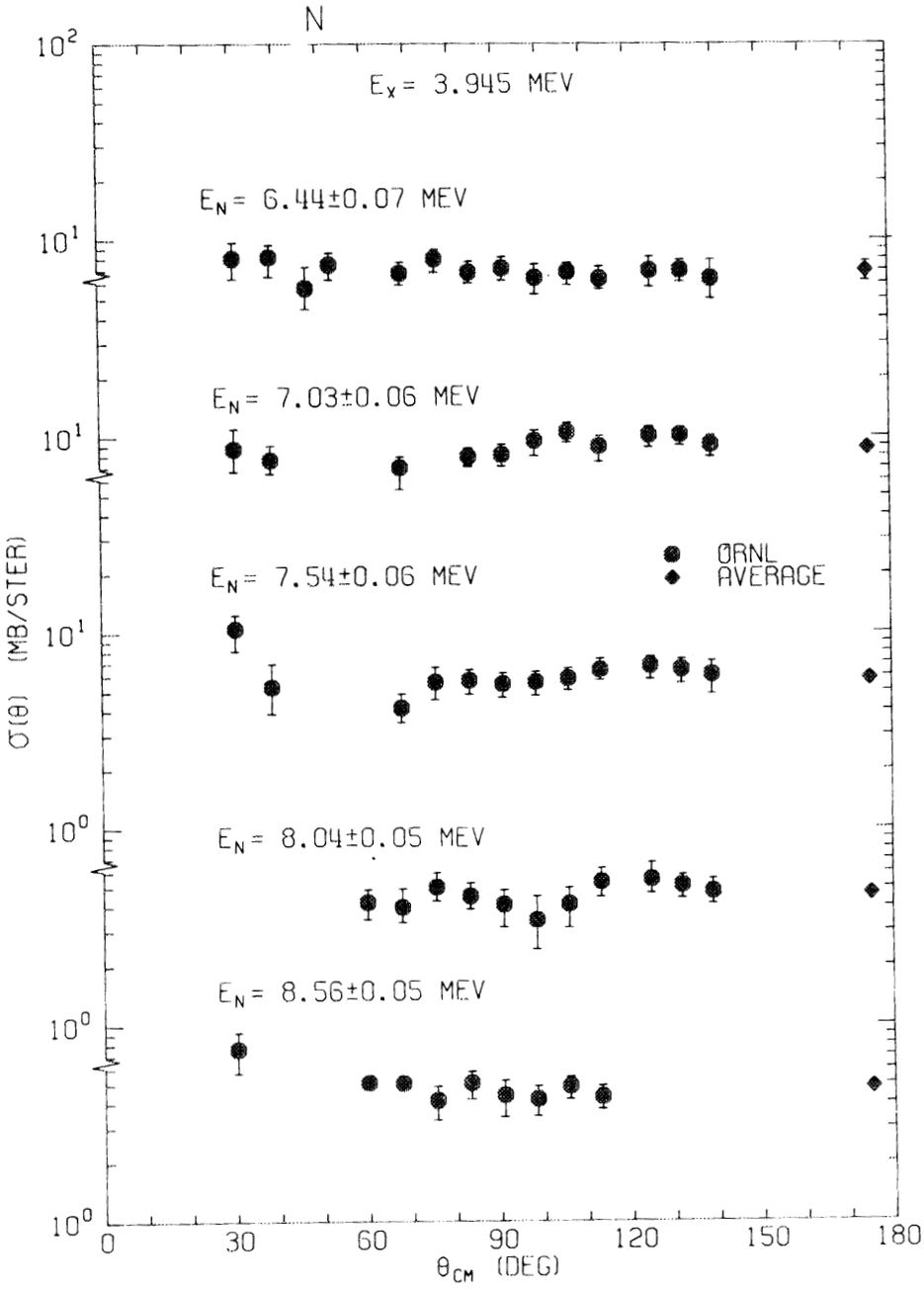

Fig. 7. Our differential center-of-mass cross sections for inelastic scattering to the 3.945 MeV level in nitrogen. The 7% uncertainty in absolute normalization common to all points is not included in the error bars.

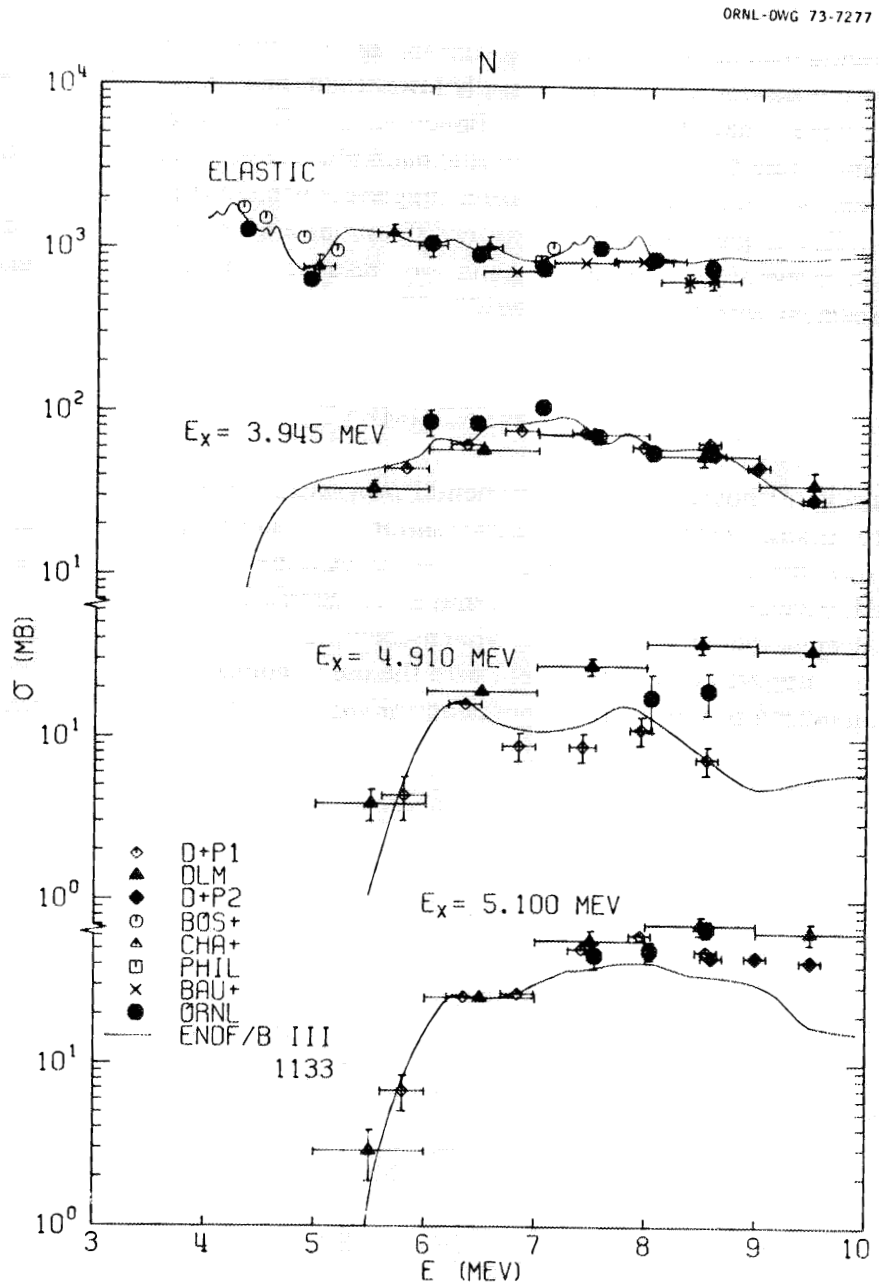

Fig. 8. Our angle-integrated differential cross sections as a function of incident neutron energy compared with the results of the investigators listed in Table I and with the results of Dickens and Perey[11] (D+P1), Dickens and Perey[12] (D+P2), and Dickens, Love, and Morgan[13] (DLM), and with ENDF/B III MAT 1133.

CONCLUSIONS

Our differential elastic scattering cross sections agree with previous results of Chase et al. and Phillips but generally are systematically lower than the results of Bostrom et al. and systematically higher than the results of Bauer et al. While resonant behavior might account for some of the differences, it can not explain all. Our elastic data do not support a "nitrogen non-elastic discrepancy" as has been suggested through the use of the elastic data of Bauer et al. Our angle-integrated inelastic differential cross sections are in reasonable agreement with previously reported gamma ray results. Our results are generally in reasonable agreement with ENDF/B III MAT 1133.

ACKNOWLEDGMENTS

Many have contributed to this experimental program at one time or another and we would like to thank them for their contributions. In particular, we would like to acknowledge the help of J. K. Dickens, J. W. McConnell, J. A. Biggerstaff, A. M. Marusak, P. H. Stelson, C. O. LeRigoleur, and E. Hungerford.

We are deeply indebted to F. C. Maienschein, director of the Neutron Physics Division, for his support of the experiment with the use of computers in report preparation and type setting which produced this report and the other six of our last seven reports.

REFERENCES

1. F. G. Perey and W. E. Kinney, "Carbon Neutron Elastic- and Inelastic-Scattering Cross Sections from 4.5 to 8.5 MeV," ORNL-4441 (December 1970).

F. G. Perey, C. O. LeRigoleur and W. E. Kinney, "Nickel-60 Neutron Elastic- and Inelastic-Scattering Cross Sections from 6.5 to 8.5 MeV," ORNL-4523 (April 1970).

W. E. Kinney and F. G. Perey, "Neutron Elastic- and Inelastic-Scattering Cross Sections from ^{56}Fe in the Energy Range 4.19 to 8.56 MeV," ORNL-4515 (June 1970).

F. G. Perey and W. E. Kinney, "Calcium Neutron Elastic- and Inelastic-Scattering Cross Sections from 4.0 to 8.5 MeV," ORNL-4519 (April 1970).

F. G. Perey and W. E. Kinney, "Sulfur Neutron Elastic- and Inelastic-Scattering Cross Sections from 4 to 8.5 MeV," ORNL-4539 (June 1970).

W. E. Kinney and F. G. Perey, "Neutron Elastic- and Inelastic- Scattering Cross Sections for Co in the Energy Range 4.19 to 8.56 MeV," ORNL-4549 (June 1970).

W. E. Kinney and F. G. Perey, "Neutron Elastic- and Inelastic- Scattering Cross Sections for Mg in the Energy Range 4.19 to 8.56 MeV," ORNL-4550 (June 1970).

W. E. Kinney and F. G. Perey, "Neutron Elastic- and Inelastic- Scattering Cross Sections for Si in the Energy Range 4.19 to 8.56 MeV," ORNL-4517 (July 1970).

F. G. Perey and W. E. Kinney, "Neutron Elastic- and Inelastic- Scattering Cross Sections for Na in the Energy Range of 5.4 to 8.5 MeV," ORNL-4518 (August 1970).

W. E. Kinney and F. G. Perey, "Al Neutron Elastic- and Inelastic- Scattering Cross Sections from 4.19 to 8.56 MeV," ORNL-4516 (October 1970).

F. G. Perey and W. E. Kinney, "V Neutron Elastic- and Inelastic- Scattering Cross Sections from 4.19 to 8.56 MeV," ORNL-4551 (October 1970).

F. G. Perey and W. E. Kinney, "Neutron Elastic- and Inelastic- Scattering Cross Sections for Yttrium in the Energy Range 4.19 to 8.56 MeV," ORNL-4552 (December 1970).

W. E. Kinney and F. G. Perey, "Neutron Elastic- and Inelastic- Scattering Cross Sections for Oxygen in the Energy Range 4.34 to 8.56 MeV," ORNL-4780 (April 1972).

W. E. Kinney and F. G. Perey, "W Neutron Elastic- and Inelastic- Scattering Cross Sections from 4.34 to 8.56 MeV," ORNL-4803 (May 1973).

W. E. Kinney and F. G. Perey, "^{238}U Neutron Elastic-Scattering Cross Sections from 6.44 to 8.56 MeV", ORNL-4804 (June 1973).

W. E. Kinney and F. G. Perey, "Natural Titanium Neutron Elastic and Inelastic Scattering Cross Sections from 4.07 to 8.56 MeV," ORNL-4810 (October 1973).

W. E. Kinney and F. G. Perey, "Natural Nickel and ^{60}Ni Neutron Elastic and Inelastic Scattering Cross Sections from 4.07 to 8.56 MeV," ORNL-4807 (November 1973).

W. E. Kinney and F. G. Perey, "Natural Chromium and ^{52}Cr Neutron Elastic and Inelastic Scattering Cross Sections from 4.07 to 8.56 MeV," ORNL-4806 (November 1973).

W. E. Kinney and F. G. Perey, "^{54}Fe Neutron Elastic and Inelastic Scattering Cross Sections from 4.34 to 8.56 MeV," ORNL-4907 (January 1974).

W. E. Kinney and F. G. Perey "^{63}Cu and ^{65}Cu Neutron Elastic and Inelastic Scattering Cross Sections from 5.50 to 8.50 MeV," ORNL-4908 (January 1974).

W. E. Kinney and F. G. Perey, "^{206}Pb, ^{207}Pb, and ^{208}Pb Neutron Elastic and Inelastic Scattering Cross Sections from 5.50 to 8.50 MeV," ORNL-4909 (To be published).

2. W. E. Kinney, "Neutron Elastic and Inelastic Scattering from ^{56}Fe from 4.60 to 7.55 MeV," ORNL-TM-2052, January 1968.

3. R. E. Textor and V. V. Verbinski, "05S: A Monte Carlo Code for Calculating Pulse Height Distributions Due to Monoenergetic Neutrons Incident on Organic Scintillators," ORNL-4160 (February 1968).

4. W. E. Kinney, Nucl. Instr. and Meth., *83*,15 (1970).

5. Norman A. Bostrom, Ira L. Morgan, J. Thomas Prud'homme, Abdul R. Sattar, "The Elastic Scattering of Fast Neutrons from Oxygen and Nitrogen," WADC Technical Report *57*-446 (September 1957)

6. L. F. Chase, Jr., R. G. Johnson, R. V. Smith, F. J. Vaughn, and M. Walt, "Fast Neutron Cross Sections of Oxygen and Nitrogen," Lockheed Aircraft Corporation Report AFSWC-TR-6115 (February 1961)

7. R. W. Bauer, J. D. Anderson, H. F. Lutz, C. Wong, J. W. McClure and B. A. Pohl, Nucl. Phys. *A93*, 673 (1967)

8. D. D. Phillips, data given in "Angular Distributions in Neutron-Induced Reactions, Volume 1, Z = 1 to 20," BNL-400, Third Edition (January 1970)

9. A. D. Carlson and R. J. Cerbone, Nucl. Sci. Eng. *42*, 28 (1970)

10. F. G. Perey and W. E. Kinney, Nucl. Sci. Eng. *46*, 428 (1971)

11. J, K. Dickens and F. G. Perey, Nucl. Sci. Eng. *36*, 280 (1969)

12. J. K. Dickens and F. G. Perey, Nucl. Sci. Eng. *40*, 346 (1970)

13. J. K. Dickens, T. A. Love, and G. L. Morgan, "Gamma-Ray Production Due to Neutron Interactions with Nitrogen for Incident Neutron Energies Between 2.0 and 20 MeV: Tabulated Differential Cross Sections," ORNL-4864 (1973).

APPENDIX

Tabulated Values of Nitrogen Neutron Elastic Scattering Cross Sections and Cross Sections for Inelastic Scattering to Discrete Levels

Our measured values for nitrogen neutron elastic scattering cross sections and cross sections for inelastic scattering to discrete levels are tabulated below. The uncertainties in differential cross sections, indicated by Δ in the tables, are relative and do *not* include a $\pm 7\%$ uncertainty in detector efficiency which is common to all points. The $\pm 7\%$ uncertainty is included in the integrated and average values.

$E_n = 4.34 \pm 0.07$ MeV
Elastic Scattering

θ_{cm} deg.	$d\sigma/d\omega$ mb/str	Δ (%) +	Δ (%) −
18.74	525.27	9.4	10.1
18.74	363.25	11.6	11.3
26.74	357.39	5.4	5.7
26.74	400.49	12.0	12.3
26.74	320.21	9.5	10.7
34.71	258.57	6.4	8.1
34.71	299.69	13.7	13.7
42.64	200.24	6.1	6.7
50.53	120.50	8.0	6.9
58.36	83.35	6.9	6.1
66.14	48.42	11.1	8.4
73.86	36.41	9.9	9.8
81.51	31.73	9.7	10.7
89.09	34.24	10.9	10.0
99.09	35.46	9.0	10.7
106.51	46.81	12.6	6.7
113.86	53.37	7.7	7.1
125.00	71.29	6.3	6.7
132.19	82.70	6.8	5.7
139.33	93.73	5.6	5.6

$\int(d\sigma/d\omega)d\omega = 1282.34$ mb $\pm$ 7.3 %

Legendre Fit, Order = 5

k	a_k	Δ(%)
0	204.09093	2.2
1	62.02466	6.5
2	68.86284	4.4
3	28.57904	9.6
4	9.55242	16.8
5	3.55062	39.9

$E_n = 4.92 \pm 0.06$ MeV
Elastic Scattering

θ_{cm} deg.	$d\sigma/d\omega$ mb/str	Δ (%) +	Δ (%) −
26.74	87.94	14.5	15.4
26.74	89.55	11.8	12.8
32.05	85.50	30.9	24.3
34.70	76.67	14.4	15.8
34.71	72.21	12.8	11.9
42.63	54.69	13.7	14.1
42.64	44.44	12.6	17.5
50.53	40.44	8.4	8.2
58.36	37.62	7.1	7.8
66.14	33.49	8.5	8.9
73.86	41.88	10.4	8.4
81.51	46.40	8.1	8.2
89.09	51.82	6.2	9.2
99.09	50.76	8.4	6.6
106.51	51.68	6.0	7.0
113.86	50.49	8.3	6.4
125.00	46.58	8.1	7.2
132.19	44.22	7.1	7.7
139.33	45.94	9.0	7.7

$\int(d\sigma/d\omega)d\omega = 642.94$ mb $\pm$ 7.5 %

Legendre Fit, Order = 5

k	a_k	Δ(%)
0	102.32669	2.7
1	7.78747	29.9
2	7.90209	22.2
3	8.21329	19.0
4	5.38686	19.8
5	0.86897	104.0

$E_n = 6.01 \pm 0.07$ MeV
Elastic Scattering

θ_{cm}	$d\sigma/d\omega$	Δ (%)	
deg.	*mb/str*	+	−
16.10	277.90	10.1	10.1
24.10	228.00	10.1	10.1
29.39	201.93	8.2	8.0
37.36	160.43	4.8	4.7
45.27	110.86	7.6	7.4
50.52	97.80	6.5	6.8
58.36	67.06	7.9	7.2
66.14	47.99	10.1	8.5
73.86	49.60	6.4	6.8
81.51	49.99	6.6	6.8
89.09	63.69	5.6	7.1
96.60	71.58	6.2	7.0
104.04	74.50	5.9	6.3
111.41	70.54	5.8	6.3
123.07	59.73	8.6	8.6
130.28	58.56	8.6	8.4
137.43	58.28	7.9	9.3

$\int(d\sigma/d\omega)d\omega = 1080.70$ mb $\pm$ 7.4 %

Legendre Fit, Order = 5

k	a_k	Δ(%)
0	171.99825	2.4
1	32.72183	11.9
2	31.69383	9.3
3	16.22054	16.5
4	9.89505	16.4
5	−3.10324	42.8

$E_n = 6.01 \pm 0.07$ MeV
(n,n′) to: 3.945 MeV Level

θ_{cm}	$d\sigma/d\omega$	Δ (%)	
deg.	*mb/str*	+	−
92.58	6.43	17.9	17.9
100.08	10.66	22.7	21.5
107.43	6.01	32.1	28.4
114.75	6.04	37.3	33.7
126.12	7.76	37.5	35.4

Avg. $d\sigma/d\omega$ = 6.96 mb/str $\pm$ 17.9 %
$\int(d\sigma/d\omega)d\omega$ = 87.41 mb $\pm$ 17.9 %

$E_n = 6.01 \pm 0.07$ MeV
(n,n′) to: 3.945 MeV Level
+ 4.910 MeV Level

θ_{cm}	$d\sigma/d\omega$	Δ (%)	
deg.	*mb/str*	+	−
84.89	8.12	24.9	18.9

Avg. $d\sigma/d\omega$ = 8.12 mb/str $\pm$ 23.0 %
$\int(d\sigma/d\omega)d\omega$ = 102.09 mb $\pm$ 23.0 %

$E_n = 6.44 \pm 0.07$ MeV
Elastic Scattering

θ_{cm}	$d\sigma/d\omega$	Δ (%)	
deg.	*mb/str*	+	−
16.06	302.84	9.5	10.6
24.07	238.45	12.6	9.3
29.39	225.05	5.0	5.1
37.35	151.12	5.4	5.8
45.27	91.59	7.4	6.3
50.53	74.76	8.2	5.0
58.36	47.76	5.1	4.8
66.14	33.17	5.4	6.5
73.85	33.46	5.9	5.9
81.51	44.08	5.4	5.2
89.09	52.29	5.6	4.6
96.60	65.36	4.2	4.9
104.04	65.41	4.4	5.0
111.42	58.59	4.8	4.9
123.07	42.46	6.5	5.4
130.28	35.21	6.1	6.4
137.43	35.90	5.8	5.7

$\int(d\sigma/d\omega)d\omega$ = 926.64 mb $\pm$ 7.4 %

Legendre Fit, Order = 6

k	a_k	Δ(%)
0	147.47894	2.3
1	40.78865	7.0
2	33.33763	7.9
3	21.25345	8.7
4	14.00822	11.6
5	−2.23108	41.3
6	−0.21372	377.7

$E_n = 6.44 \pm 0.07$ MeV
(n,n′) to: 3.945 MeV Level

θ_{cm}	$d\sigma/d\omega$	Δ (%)	
deg.	*mb/str*	+	−
30.72	8.07	20.5	21.8
38.99	8.16	15.8	20.8
47.22	5.70	28.0	22.0
52.66	7.48	15.0	16.4
68.70	6.75	13.7	13.2
76.59	7.96	11.9	14.7
84.35	6.81	13.6	12.0
91.99	7.12	14.3	13.3
99.49	6.37	17.2	17.6
106.90	6.81	11.0	14.4
114.20	6.29	15.2	11.8
125.60	6.88	18.1	17.2
132.59	6.92	12.8	12.9
139.54	6.28	24.6	21.1

Avg. $d\sigma/d\omega$ = 6.89 mb/str ± 11.3 %
$\int(d\sigma/d\omega)d\omega$ = 86.59 mb ± 11.3 %

$E_n = 7.03 \pm 0.06$ MeV
Elastic Scattering

θ_{cm}	$d\sigma/d\omega$	Δ (%)	
deg.	*mb/str*	+	−
29.39	167.34	6.4	6.6
37.35	121.23	6.3	6.0
45.30	80.37	7.1	7.1
50.52	56.97	5.4	7.0
58.36	31.86	7.0	10.1
66.14	18.17	8.1	7.7
73.80	19.19	8.4	8.4
81.50	26.85	6.9	7.0
89.09	38.23	7.3	5.5
96.60	52.32	5.6	5.5
104.04	62.03	5.5	5.4
111.41	61.51	5.4	4.8
123.07	57.34	5.8	5.1
130.28	44.31	5.2	5.8
137.43	38.60	5.5	6.4

$\int(d\sigma/d\omega)d\omega$ = 769.32 mb ± 7.7 %

Legendre Fit, Order = 6

k	a_k	Δ(%)
0	122.44165	3.2
1	26.61214	11.8
2	26.97581	11.5
3	22.00331	9.7
4	9.07875	20.7
5	−2.70384	36.8
6	0.88281	98.3

$E_n = 7.03 \pm 0.06$ MeV
(n,n′) to: 3.945 MeV Level

θ_{cm} deg.	$d\sigma/d\omega$ mb/str	Δ (%) +	Δ (%) −
30.50	8.71	27.1	23.4
38.73	7.64	18.5	14.8
68.27	6.98	13.4	23.1
83.86	7.90	10.7	10.7
91.49	8.07	12.9	12.7
99.01	9.47	13.5	16.4
106.44	10.47	11.9	11.3
113.72	8.86	13.1	16.7
125.17	10.09	10.9	13.3
132.20	10.14	9.4	12.1
139.15	9.01	11.5	13.2

Avg. $d\sigma/d\omega$ = 8.66 mb/str ± 9.8 %
$\int(d\sigma/d\omega)d\omega$ = 108.86 mb ± 9.8 %

$E_n = 7.03 \pm 0.06$ MeV
(n,n′) to: 4.910 MeV Level
+ 5.100 MeV Level

θ_{cm} deg.	$d\sigma/d\omega$ mb/str	Δ (%) +	Δ (%) −
86.13	3.97	28.4	26.8
93.82	3.18	45.2	34.7
101.37	6.27	0.0	25.5
108.75	5.05	41.4	28.4
115.96	4.52	39.6	33.1
127.08	4.76	35.9	34.5
134.00	3.87	50.8	40.3

Avg. $d\sigma/d\omega$ = 4.52 mb/str ± 28.6 %
$\int(d\sigma/d\omega)d\omega$ = 56.85 mb ± 28.6 %

$E_n = 7.54 \pm 0.06$ MeV
Elastic Scattering

θ_{cm} deg.	$d\sigma/d\omega$ mb/str	Δ (%) +	Δ (%) −
16.06	494.41	7.4	7.4
24.07	328.55	8.2	8.1
29.39	251.25	5.5	5.2
37.35	136.37	6.3	6.2
45.27	67.11	7.3	7.2
50.52	42.39	5.7	5.5
58.36	24.56	6.6	7.5
66.14	24.81	6.2	6.2
73.85	36.52	5.3	6.2
81.50	53.28	5.1	4.9
89.09	58.18	4.7	4.7
96.60	67.32	4.8	4.5
104.04	64.44	4.4	4.7
111.41	58.62	5.1	5.2
123.07	55.11	4.9	6.2
130.28	52.02	5.5	5.9
137.43	52.45	5.1	5.3

$\int(d\sigma/d\omega)d\omega$ = 1026.16 mb ± 7.4 %

Legendre Fit, Order = 7

k	a_k	Δ(%)
0	163.31798	2.5
1	46.88577	8.1
2	47.05290	6.8
3	37.39906	7.3
4	25.58768	7.3
5	8.71722	17.7
6	2.47646	34.4
7	1.07458	72.8

$E_n = 7.54 \pm 0.06$ MeV
(n,n′) to: 3.945 MeV Level

θ_{cm} deg.	$d\sigma/d\omega$ mb/str	Δ (%) +	Δ (%) −
30.35	10.53	18.2	23.3
38.55	5.29	31.4	27.0
68.01	4.14	18.4	15.6
75.81	5.60	19.4	18.7
83.56	5.70	13.7	14.8
91.16	5.47	13.8	14.6
98.69	5.58	13.3	14.7
106.10	5.81	12.9	12.7
113.42	6.42	14.2	11.5
124.89	6.74	11.1	14.9
131.96	6.46	12.8	15.4
138.92	6.07	17.3	20.4

Avg. $d\sigma/d\omega$ = 5.77 mb/str ± 9.2 %
$\int(d\sigma/d\omega)d\omega$ = 72.55 mb ± 9.2 %

$E_n = 7.54 \pm 0.06$ MeV
(n,n′) to: 4.910 MeV Level
+ 5.100 MeV Level

θ_{cm} deg.	$d\sigma/d\omega$ mb/str	Δ (%) +	Δ (%) −
100.42	2.41	24.6	0.0

Avg. $d\sigma/d\omega$ = 2.41 mb/str ± 25.6 %
$\int(d\sigma/d\omega)d\omega$ = 30.25 mb ± 25.6 %

$E_n = 7.54 \pm 0.06$ MeV
(n,n′) to: 5.100 MeV Level

θ_{cm} deg.	$d\sigma/d\omega$ mb/str	Δ (%) +	Δ (%) −
92.89	4.75	19.6	23.8
100.44	3.67	24.5	21.0
107.77	3.05	29.9	27.8

Avg. $d\sigma/d\omega$ = 3.71 mb/str ± 17.7 %
$\int(d\sigma/d\omega)d\omega$ = 46.57 mb ± 17.7 %

$E_n = 8.04 \pm 0.05$ MeV
Elastic Scattering

θ_{cm} deg.	$d\sigma/d\omega$ mb/str	Δ (%) +	Δ (%) −
29.39	219.97	7.4	6.0
37.35	121.64	6.5	7.1
45.31	57.59	7.6	8.9
50.52	36.63	6.8	7.1
58.36	24.29	7.0	7.5
66.14	29.27	6.5	5.8
73.85	43.10	5.7	5.5
81.50	55.02	4.7	5.6
89.09	60.58	4.7	5.0
96.60	54.90	6.8	5.9
104.04	55.60	5.4	5.6
111.41	43.01	7.8	7.5
123.07	37.54	6.4	6.2
130.28	36.89	6.8	5.5
137.42	37.38	5.5	6.3

$\int(d\sigma/d\omega)d\omega$ = 883.04 mb ± 7.9 %

Legendre Fit, Order = 7

k	a_k	Δ(%)
0	140.54095	3.6
1	43.74666	10.7
2	37.48164	10.6
3	28.92120	11.8
4	23.43137	10.0
5	7.81744	23.9
6	1.61394	64.0
7	0.02767	3088.3

$E_n = 8.04 \pm 0.05$ MeV
(n,n′) to: 3.945 MeV Level

θ_{cm} deg.	$d\sigma/d\omega$ mb/str	Δ (%) +	Δ (%) −
59.88	4.22	15.7	18.4
67.78	3.97	24.4	16.5
75.59	5.02	18.8	15.0
83.30	4.51	17.0	13.9
90.93	4.09	18.5	23.4
98.45	3.41	32.4	29.1
105.87	4.11	21.2	24.5
113.21	5.32	17.8	16.3
124.68	5.50	21.7	15.3
131.76	5.12	13.0	14.2
138.75	4.75	16.2	13.6

Avg. $d\sigma/d\omega$ = 4.62 mb/str ± 9.5 %
$\int(d\sigma/d\omega)d\omega$ = 58.01 mb ± 9.5 %

$E_n = 8.04 \pm 0.05$ MeV
(n,n′) to: 4.910 MeV Level

θ_{cm} deg.	$d\sigma/d\omega$ mb/str	Δ (%) +	Δ (%) −
106.89	1.43	36.2	40.1

Avg. $d\sigma/d\omega$ = 1.43 mb/str ± 38.8 %
$\int(d\sigma/d\omega)d\omega$ = 18.02 mb ± 38.8 %

$E_n = 8.04 \pm 0.05$ MeV
(n,n′) to: 4.910 MeV Level
+ 5.100 MeV Level

θ_{cm} deg.	$d\sigma/d\omega$ mb/str	Δ (%) +	Δ (%) −
68.93	3.10	18.6	18.6

Avg. $d\sigma/d\omega$ = 3.10 mb/str ± 19.9 %
$\int(d\sigma/d\omega)d\omega$ = 38.89 mb ± 19.9 %

$E_n = 8.04 \pm 0.05$ MeV
(n,n′) to: 5.100 MeV Level

θ_{cm} deg.	$d\sigma/d\omega$ mb/str	Δ (%) +	Δ (%) −
68.93	2.94	20.7	20.7
76.85	4.03	20.9	36.9
84.59	3.20	24.8	22.1
92.27	4.02	17.0	25.0
107.17	5.56	23.0	19.1
114.47	6.20	17.4	27.7
125.81	5.53	19.6	17.9

Avg. $d\sigma/d\omega$ = 3.97 mb/str ± 12.6 %
$\int(d\sigma/d\omega)d\omega$ = 49.83 mb ± 12.6 %

$E_n = 8.04 \pm 0.05$ MeV
(n,n′) to: 5.690 MeV Level

θ_{cm} deg.	$d\sigma/d\omega$ mb/str	Δ (%) +	Δ (%) −
77.85	2.11	37.1	40.8
85.58	2.01	30.5	34.7
93.35	1.67	35.4	35.9

Avg. $d\sigma/d\omega$ = 1.87 mb/str ± 23.1 %
$\int(d\sigma/d\omega)d\omega$ = 23.54 mb ± 23.1 %

$E_n = 8.04 \pm 0.05$ MeV
(n,n′) to: 5.830 MeV Level

θ_{cm} deg.	$d\sigma/d\omega$ mb/str	Δ (%) +	Δ (%) −
78.30	6.04	21.4	31.3
86.07	6.16	16.3	16.1
93.77	6.04	15.7	25.3

Avg. $d\sigma/d\omega$ = 6.09 mb/str ± 13.5 %
$\int(d\sigma/d\omega)d\omega$ = 76.47 mb ± 13.5 %

$E_n = 8.56 \pm 0.05$ MeV
Elastic Scattering

θ_{cm} deg.	$d\sigma/d\omega$ mb/str	Δ (%) +	Δ (%) −
24.07	303.89	9.0	9.2
29.39	192.64	6.9	6.1
37.35	119.93	7.2	6.5
45.28	62.80	8.7	6.7
50.52	49.22	5.1	4.2
58.36	24.59	4.8	5.7
66.14	18.88	6.2	6.1
73.86	26.73	7.1	6.5
81.50	38.77	5.2	5.2
89.09	49.70	5.5	5.2
96.60	57.13	5.1	4.1
104.04	55.68	4.4	4.2
111.41	50.53	4.9	4.4
123.07	34.59	6.9	7.4
130.27	21.14	7.5	7.9
137.42	22.75	7.6	9.1

$\int(d\sigma/d\omega)d\omega = 787.08$ mb $\pm$ 7.6 %

Legendre Fit, Order = 7

k	a_k	Δ(%)
0	125.26854	3.0
1	41.54575	8.6
2	33.57846	8.9
3	26.36707	9.8
4	19.54556	8.9
5	1.58617	91.3
6	1.22309	63.7
7	0.95945	71.0

$E_n = 8.56 \pm 0.05$ MeV
(n,n′) to: 3.945 MeV Level

θ_{cm} deg.	$d\sigma/d\omega$ mb/str	Δ (%) +	Δ (%) −
30.15	7.59	21.6	24.6
59.73	5.10	8.7	8.4
67.61	5.06	8.3	10.7
75.41	4.14	17.7	20.7
83.13	5.06	14.7	17.3
90.74	4.38	19.2	22.3
98.27	4.18	17.1	17.8
105.69	4.86	12.0	14.2
113.00	4.29	13.9	13.6

Avg. $d\sigma/d\omega$ = 4.79 mb/str $\pm$ 9.2 %
$\int(d\sigma/d\omega)d\omega$ = 60.16 mb $\pm$ 9.2 %

$E_n = 8.56 \pm 0.05$ MeV
(n,n′) to: 4.910 MeV Level

θ_{cm} deg.	$d\sigma/d\omega$ mb/str	Δ (%) +	Δ (%) −
99.14	1.59	29.6	27.3

Avg. $d\sigma/d\omega$ = 1.59 mb/str $\pm$ 29.3 %
$\int(d\sigma/d\omega)d\omega$ = 19.96 mb $\pm$ 29.3 %

$E_n = 8.56 \pm 0.05$ MeV
(n,n′) to: 5.100 MeV Level

θ_{cm} deg.	$d\sigma/d\omega$ mb/str	Δ (%) +	Δ (%) −
91.83	5.65	18.4	23.6
99.35	5.26	12.8	15.6
114.03	5.49	14.0	12.8

Avg. $d\sigma/d\omega$ = 5.40 mb/str $\pm$ 11.8 %
$\int(d\sigma/d\omega)d\omega$ = 67.86 mb $\pm$ 11.8 %

ORNL-4805
UC-79d
(ENDF-205)

INTERNAL DISTRIBUTION

1–3. Central Research Library
4. ORNL – Y-12 Technical Library Document Reference Section
5–24. Laboratory Records Department
25. Laboratory Records, ORNL R.C.
26–28. L. S. Abbott
29. R. G. Alsmiller, Jr.
30. C. E. Clifford
31. F. L. Culler
32. J. K. Dickens
33. C. Y. Fu
34. W. O. Harms
35. R. F. Hibbs
36–45. W. E. Kinney
46. T. A. Love
47–48. F. C. Maienschein
49. G. L. Morgan
50. F. R. Mynatt
51. E. M. Oblow
52. R. W. Peelle
53. S. K. Penny
54–68. F. G. Perey
69. Herman Postma
70. R. W. Roussin
71. M. J. Skinner
72. A. M. Weinberg
73. A. Zucker
74. H. Feshbach (Consultant)
75. P. F. Fox (Consultant)
76. W. W. Haven, Jr. (Consultant)
77. A. F. Henry (Consultant)

EXTERNAL DISTRIBUTION

78–79. USAEC Division of Reactor Research and Development, Washington, D.C. 20545
80. USAEC-RRD Senior Site Representative, ORNL
81. Research and Technical Support Division, AEC, ORO
82. Patent Office, AEC, ORO
83–309. Given distribution as shown in TID-4500 under UC-79d, Liquid Metal Fast Breeder Reactors (Physics)
310–369. Technical Information Center for ENDF distribution